Oncogene
https://doi.org/10.1038/s41388-020-01506-6

ARTICLE

Tenascin C promotes cancer cell plasticity in mesenchymal glioblastoma

Inbar Angel[1] · Ori Pilo Kerman[1] · Liat Rousso-Noori[1] · Dinorah Friedmann-Morvinski[1,2]

Received: 6 January 2020 / Revised: 17 September 2020 / Accepted: 1 October 2020

Abstract

Interconversion of transformed non-stem cells to cancer stem cells, termed cancer cell plasticity, contributes to intra-tumor heterogeneity and its molecular mechanisms are currently unknown. Here, we have identified Tenascin C (TNC) to be upregulated and secreted in mesenchymal glioblastoma (MES GBM) subtype with high NF-κB signaling activity. Silencing TNC decreases proliferation, migration and suppresses self-renewal of glioma stem cells. Loss of TNC in MES GBM compromises de-differentiation of transformed astrocytes and blocks the ability of glioma stem cells to differentiate into tumor derived endothelial cells (TDEC). Inhibition of NF-κB activity or TNC knockdown in tumor cells decreased their tumorigenic potential in vivo. Our results uncover a link between NF-κB activation in MES GBM and high levels of TNC in GBM extracellular matrix. We suggest that TNC plays an important role in the autocrine regulation of glioma cell plasticity and hence can be a potential molecular target for MES GBM.

Introduction

Glioblastoma (GBM) is the most common and deadliest type of human primary brain cancers and remains an incurable tumor [1]. Despite standard of care treatment protocols, which consist of surgery, followed by radiation therapy and/or chemotherapy, patients diagnosed with GBM have an average survival of 15 months from the time of diagnosis. Lack of effective therapeutic options has been attributed to one of the most important hallmarks of GBM: tumor heterogeneity. There are multiple levels of heterogeneity, with intertumor heterogeneity mostly associated with genetic alterations and molecular variations found in different patients diagnosed with GBM [2]. These molecular differences, so called molecular signatures, allow the classification of GBM in different subtypes [3, 4]. Intratumor heterogeneity can also be attributed to molecular differences that occur within the same tumor, but the complexity of intratumor heterogeneity can go beyond genetic alterations. Phenotypic and functional heterogeneity defined by subpopulations of neoplastic cells with diverse functional properties and expressing different lineage markers, irrespective of their genetic alteration, can reside in distinct states of cellular differentiation [5]. The ability of cancer cells to interconvert from a non-cancer stem cell-state (CSC) to a CSC has been reported previously under different conditions [6–9], and in GBM we have previously shown that tumors can originate from oncogenic transduction of terminally differentiated astrocytes and neurons [10]. We proposed that these transformed cells could undergo de-differentiation from a more mature state to a cancer stem/progenitor like state, generating very heterogeneous glioma tumors. The plasticity of GBM cells not only contributes to tumor maintenance, progression and invasion, but also facilitates the formation of its own blood vessels by generating tumor derived endothelial cells [11].

The mechanisms that confer this reversible and dynamic plasticity between cancer stem cell state and differentiated cancer cell state remain poorly understood. Cumulative evidence suggests that multiple different intrinsic and extrinsic factors may contribute to this process. The tumor

Supplementary information The online version of this article (https://doi.org/10.1038/s41388-020-01506-6) contains supplementary material, which is available to authorized users.

✉ Dinorah Friedmann-Morvinski
dino@tauex.tau.ac.il

[1] School of Neurobiology, Biochemistry and Biophysics, The George S. Wise Faculty of Life Sciences, Tel Aviv University, Tel Aviv-Yafo, Israel

[2] Sagol School of Neuroscience, Tel Aviv University, Tel Aviv-Yafo, Israel

Published online: 19 October 2020

microenvironment and its non-cellular component, the extracellular matrix (ECM), have been shown to contribute to many important aspects of tumor initiation and progression, creating a niche that supports tumor growth. Tumor cells have the capacity to overexpress and secrete different molecules and matrix components to shape their own ECM [12].

Tenascin-C (TNC) is an extracellular matrix glycoprotein highly expressed during embryogenesis, supporting cell proliferation and migration and participating in epithelial-mesenchymal transition (EMT), but is hardly expressed in adult tissues [13]. De novo expression of TNC can be found in stem cell niches and tendons [14], and in pathological lesions undergoing remodeling such as inflammation, wound repair and cancer [15–17]. High levels of TNC expression in the tumor microenvironment correlate with poor prognosis in different types of cancer. Due to the ability of TNC to bind several receptors and interact with multiple proteins, it has been shown to participate in multiple events in cancer such as proliferation, invasion, migration and metastasis [18]. While stromal fibroblasts are the main source of TNC in most solid tumors, in brain tumors, the tumor cells themselves secrete TNC to the tumor extracellular matrix. As one of the major components of GBM extracellular matrix, TNC has been shown to affect ECM stiffness and tumor invasion [19], which correlate with tumor grade and aggressiveness, contribute to tumor proliferation, support the growth and maintenance of glioma stem cells and exert a pro-angiogenic effects [20].

Here, we demonstrated that TNC expression correlates with mesenchymal GBM subtype and that its function is essential for proliferation, migration and maintenance of cancer stem cell self-renewal. Using a lentiviral-induced MES GBM mouse model and patient derived xenografts, we further identified a novel and autocrine role of TNC in glioma cell plasticity, and in the generation of tumor derived endothelial cells (TDEC) through activation of the NOTCH signaling pathway and the up-regulation and secretion of the pro-angiogenic EphrinB2 signaling axis. Furthermore, we show a link between NF-κB constitutive activation in MES GBM, TNC expression, and tumor cell plasticity.

Materials and methods

Cell culture

AGR53 cells (transformed primary astrocytes with HRas-shp53 lentivirus) were maintained in Dulbecco's modified Eagle's medium containing 10% fetal bovine serum. Following transduction with lentivirus, cells were either cultured in the same medium or cultured in NSCs medium containing FGF-2 and EGF. 005 is a murine glioma stem cell line generated from a lentiviral HRasV12 induced tumor in a p53-/- knockout mouse [21] and NF53-10 are murine glioma stem cells generated by transduction of NSCs with lentivirus expressing shRNAs targeting NF1, p53 and PTEN (see Table S1). Both cell lines were cultured in N2-supplemented (Invitrogen) DME:Ham's F12 (Gibco) medium containing 20 ng/ml fibroblast growth factor-2 (PeproTech), 20 ng/ml epidermal growth factor (Promega) and 40 µg/ml heparin (Sigma). U87 human glioma cell line was maintained in Dulbecco's modified Eagle's medium containing 10% fetal bovine serum. GBM1005 patient derived mesenchymal glioma stem cells (a gift from Dr. Ichiro Nakano, University of Alabama at Birmingham) were maintained in DMEM/F12/Glutamax supplemented with B27 (Gibco), 20 ng/ml fibroblast growth factor-2, 20 ng/ml epidermal growth factor and heparin (2.5 ug/ml). All cell lines were routinely tested for mycoplasma using the EZ-PCR-Mycoplasma test kit (Biological Industries).

Mice, lentiviral injections and orthotopic transplantation

hGFAP-Cre, Nestin-Cre and SynI-Cre transgenic mice were purchased from the Jackson Laboratories. C57Bl/6 and Nude 7–8 weeks old female mice were purchased from Envigo Jerusalem Israel. All experiments involving animals were approved by the Tel Aviv University Institutional Animal Care and Use Committee.

Lentivirus (HRas-shp53 or shNF1-shp53 [10]); or cells (3×10^5 cells per mouse) were stereotaxically injected into the hippocampus of 8 weeks old mice (coordinates: AP = −2.0, ML = −1.5, DV = 2.3). shRNA hairpins were cloned into an NheI site of the p156RRLsin vector [22]. See Table S2 for shRNA sequences used in this study.

NBDwt and NBDmut peptides [Nemo binding domain peptide; American Peptide Company, Sunnyvale, CA, USA] were dissolved in saline. The sequence of these peptides was previously reported [23]. NBDwt treated mice were administered 10 mg/kg intraperitoneally daily for a period of 20 days. Control vehicle group received only saline intraperitoneally.

To achieve inducible silencing of human TNC we used the Tet-regulated miR30-shRNA technology [24] (human shTNC: 5'- CCAGTGACAACATCGCAATAG-3'), combined with expression of the transactivator (m2RtTA) under the EF1α promoter (one single vector).

Microarray, RNAseq and bioinformatics analysis

RNA was extracted from harvested cells or tumors from mice that reached end point using Trizol (Invitrogen) or RNeasy kit according to manufacturer's protocol with the

addition of DNase (Qiagen). Microarray and RNAseq protocols were described previously [10, 25].

Sequence reads were mapped to the mm9 mouse genome build. Raw reads of each individual gene were counted and normalized to fpkm using Cuffdiff v2.1.1. NF-kappaB target gene list was obtained from http://bioinfo.lifl.fr/NF-KB/. Heatmap was drawn with heatmap.2 from R package. GEO datasets: GSE73127, GSE64411, GSE35917.

qRT-PCR analysis

Total RNA extracted from murine or human cell lines or isolated from homogenized tumor samples, was reverse transcribed using qScript cDNA Synthesis kit (Quantas Biosciences). qPCR reactions were carried out with the StepOnePlus Real Time PCR System using the Fast SYBER green Master Mix (ThermoFisher scientific). Data are presented after normalization with Cyclophilin and GAPDH for mouse and 18 s for human samples. The primers used in this study are listed in Table S3.

Western blotting

Protein lysates were obtained by lysing the cells using NP-40 lysis buffer supplemented with protease inhibitors (Roche). The antibodies used are listed in Table S4.

Proliferation

Cell proliferation was measured using the WST-1 reagent from Roche. Cells were seeded at 1×10^4–2.5×10^4 cells per well in a 96-well plate in triplicates. WST-1 reagent was added to the wells and following 30 min incubation the absorbance was measured at 450 nm. Proliferation was also monitored in real time using the IncuCyte® Live cell analysis imaging system.

Flow cytometry and immunofluorescence staining

For cell cycle analysis cells were fixed with 70% cold ethanol and stained with DAPI (10 µg/ml). Apoptosis was also assessed with Annexin V (APC) and DAPI staining.

For endothelial cell staining, brain tumors were dissociated using a Neural Dissociation Kit (Miltenyi Biotec) followed by depletion of CD45+ cells using mouse CD45 MicroBeads (Miltenyi Biotec). The CD45- fraction was stained with anti-mouse CD45 (to confirm depletion) and anti-mouse CD31 antibody. Cells were analyzed on Attune NxT Instrument using Kaluza software. For fluorescent staining, coronal sections (40 µm) were cut on a microtome and images were obtained using a confocal laser-scanning microscope (Zeiss LSM880). All the antibodies are listed in Table S4.

Tube formation assay

005 cells were first induced to differentiate to endothelial cells in EGM-2 media (Lonza) with the addition of 100 µg/mL DFO mesylate (Sigma) to reproduce hypoxic conditions. Next the cells were seeded on Matrigel (Beckton Dickinson) in the absence (control) or presence of either 10 µM DAPT γ-secretase inhibitor (Sigma) [26], 500 nM EphB4 inhibitor NVP-BGH712 (Sigma) or 50 µM of NBD peptide (NF-κB inhibitor; American Peptide Company, Sunnyvale, CA, USA) [23]. After 4–6 h. incubation, images of the cells were taken using an inverted fluorescent microscope (Nikon Eclipse Ti-S).

Limiting dilution neurosphere forming assay

005-EV and 005-shTNC tumor spheres were dissociated and seeded into 96-well plate in N2 complete media (1–100 cells per well). After 7 days, the cells were examined under the microscope for the formation of tumorspheres. The frequency of neurosphere formation was calculated using the extreme limiting dilution analysis (http://bioinf.wehi.edu.au/software/elda/).

Statistics

In vitro experiments were repeated two-three times with three technical replicates per experiment. The in vivo experiments were performed twice (the number of mice is indicated in the legend for each experiment). Statistical analysis and graphing were performed using GraphPad Prism 7.0 software for MAC. Data were analyzed using the Student's t-test and considered significant when p value was < 0.05. All statistical tests were two-sided. Log-rank analysis was used to determine statistical significance of Kaplan–Meier survival plots.

Results

TNC is overexpressed in MES GBM

Using a lentiviral-induced GBM mouse model we have previously shown that tumors derived from astrocytic and neuronal origin exhibit a strong mesenchymal (MES) molecular signature [10]. Mesenchymal GBM differentiation is mediated by NF-κB [27], and indeed, RNAseq and microarray analysis of our MES GBM murine tumors confirmed high NF-κB activation, and revealed *TNC* as one of the most upregulated genes in MES GBM and one of the top NF-κB target genes (Fig. 1a, b, in 1b tumor samples are highlighted in grey and normal brain tissue in orange). MES subtype has been linked to de-differentiated tumors and

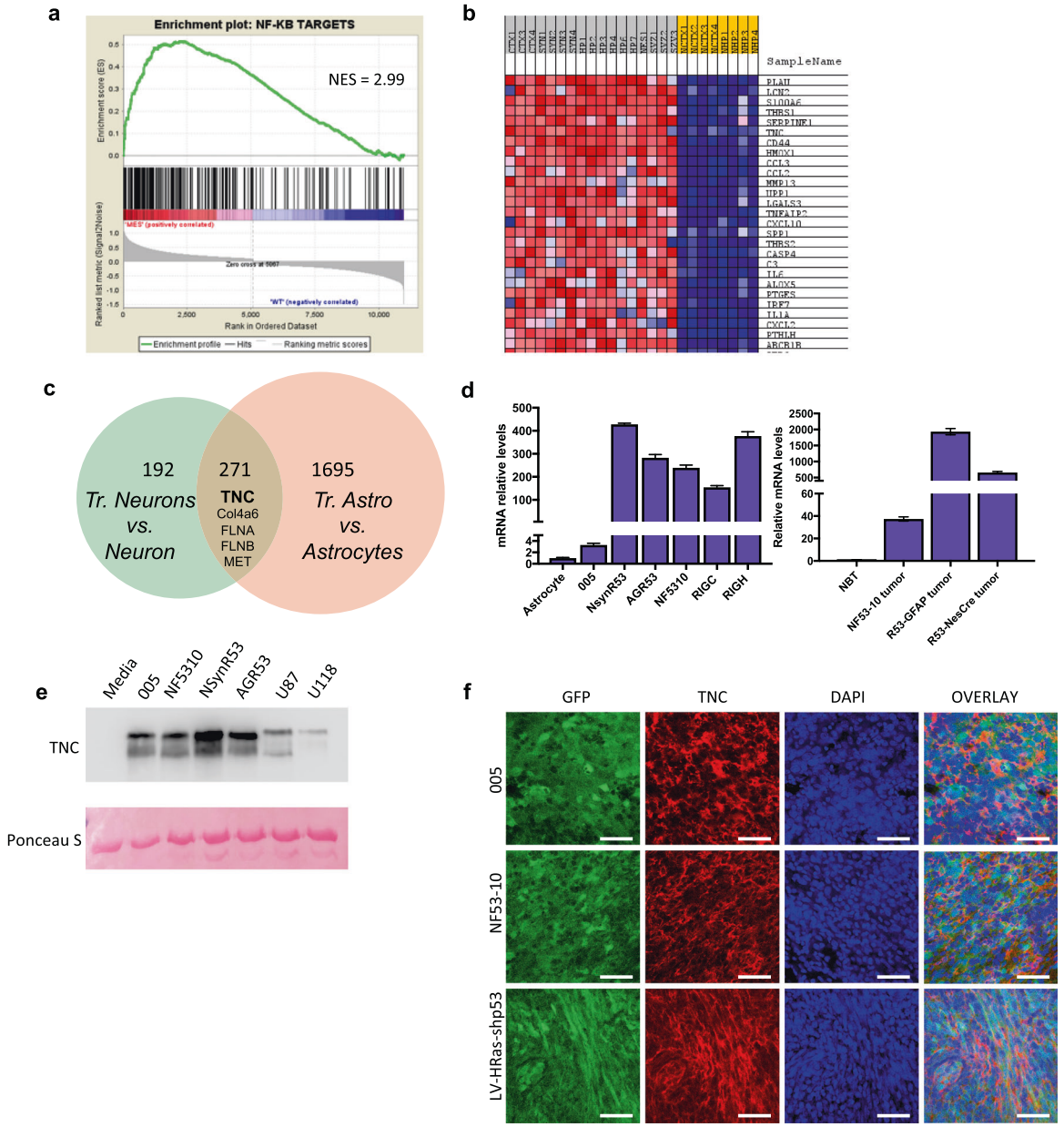

Fig. 1 TNC is overexpressed in lentiviral-induced MES GBM mouse model. a Gene set enrichment analysis (GSEA) plot of NF-κB target gene signature in MES GBM compared to normal brain tissue. Gene expression data were obtained by cDNA microarray of MES GBM and a list of NF-κB target genes (http://bioinfo.lifl.fr/NF-KB/). The normalized enrichment score (NES) is shown in the plot. **b** Heatmap of differentially expressed NF-κB target genes in MES tumors (gray label) and normal brain tissue (orange label). Heatmap colors red, white, and blue represent up-regulation, no relative effect, and down-regulation of transcripts, respectively. **c** Pathway enrichment. The genes commonly upregulated in the de-differentiated cell types (Transformed neurons (Tr. Neurons) and transformed Astro (Trs. Astrocytes) compared to their normal parental cells (neurons and astrocytes, respectively) showed enrichment for focal adhesion pathways genes. **d** qRT-PCR validation of TNC expression in both murine GBM-derived cell lines (left panel) and tumor tissue (right panel; $n = 3$ for NBT and $n = 5$ for tumors). NBT normal brain tissue. Results are normalized to the cyclophilin. Data represent fold change from control. **e** Immunoblotting for TNC in condition media from the indicated murine and human GBM cell lines. Ponceau S -stained blot was used as control for equal protein loading. **f** Immunofluorescence staining of TNC in murine MES GBM (005 and NF5310) transplanted models and lentiviral-induced GBM (LV-HRas-shp53). GFP reporter is expressed in tumor cells. Scale bar = 50 μm.

cancer plasticity [4, 28, 29]. We have previously shown that oncogenic transformation of neurons and astrocytes can induce MES glioma in mice [10]. Differential gene expression analysis of these de-differentiated transformed cells in comparison with their parental mature neurons and astrocytes identified 271 upregulated genes. Pathway enrichment analysis revealed that *TNC* was the most upregulated gene in the focal adhesion pathway (Fig. 1c and Fig. S1).

We further validated the expression levels of *TNC* in MES murine GBM cell lines and tumors by qRT-PCR (Fig. 1d) and secretion of TNC in condition media of both murine and human GBM cell lines (Fig. 1e). Confocal microscopy analysis showed expression of TNC in the tumor area (Fig. 1f and Fig. S2). The Cancer Genome Atlas (TCGA) and The Repository of Molecular Brain Neoplasia Data (REMBRANDT) showed high expression of *TNC* in glioblastoma compared to other types of gliomas and specifically upregulated in MES subtype (Figs. S3a, b). *TNC* expression is positively correlated with the expression of MES markers such as *STAT3*, *TGFB1* and *CD44*, while its expression negatively correlates with proneural (PN) markers, *OLIG2*, *DLL3* and *ASCL1* (Fig. S3c). Taken together, these data indicate that TNC is overexpressed in MES GBM.

Silencing TNC impairs cell proliferation and migration, induces apoptosis, and reduces neurosphere formation

In order to understand the functional role of TNC in glioma cell plasticity we silenced the expression of TNC in 005 glioma stem cells, derived from a MES lentiviral induced mouse model [21, 23], and AGR53 cells (transformed astrocytes, [25]), using lentiviral vectors expressing shRNA. Cells were transduced with three different individual short hairpin RNAs designed for targeting *TNC* (shTNC); shTNC1 was the most effective in suppressing the TNC protein expression and *TNC* mRNA levels (Figs. 2a, S4a, b). Since both the empty vector (EV) and the control non-targeting shRNA (shIRR) had the same effects on TNC expression (Fig. S4b–d), in the next experiments we used either one of them. TNC silencing impaired cell proliferation, measured by a metabolic activity assay and monitored by analyzing the occupied area (% confluence) of cell images over time (Fig. 2b and c). Wound-scratch assay following live imaging also revealed decreased cell migration of AGR53-shTNC cells (Fig. 2d). To further examine whether silencing *TNC* decreases the growth of glioma cells through induction of apoptosis we performed cell cycle analysis and Annexin V/Dapi double staining followed by flow cytometry analysis. Silencing TNC increased the percentage of SubG0/G1 population (apoptotic cells) from 1.4% in controls to 14.01% in AGR53-shTNC, and increased the percentage of apoptotic cells assessed by AnnexinV staining, from 4.56% in control to 9.89% and 15.6% in 005-shTNC1 and 005-shTNC3 cells, respectively (Fig. 2e, f). Neurospheres formation is an important characteristic of glioma stem cells. To assess whether *TNC* knockdown has any effect on neurospheres formation, we dissociated 005-shTNC cells, and 005-EV and 005-shIRR control tumorspheres, and re-plated the cells in their stem cell media. After 48 h, images were taken and the number of spheres was counted. We observed more neurospheres in the 005-EV and 005-shIRR control cells compared to 005-shTNC cells (Fig. 2g). Next, we analyzed the frequency of spheres formation (self-renewal capacity) using a limiting dilution sphere-forming assay, and found lower stem cell frequency for 005-shTNC cells compared to 005-EV control (Fig. 2h). Collectively, these data suggest that silencing TNC attenuates proliferation of MES glioma cells in vitro and the ability of glioma stem cells to form typical neurospheres.

TNC is required for glioma cell plasticity

To assess the possible role of TNC in glioma cell de-differentiation, we knockdown the expression of TNC in primary transformed astrocytes (AGR53 cells). To test the ability of AGR53 to de-differentiate in vitro, we switched the cell culture media from DMEM + 10%FBS media, which supports and maintains astrocytes growth, to stem cell media devoid of serum and supplemented with FGF-2 [10, 25]. While AGR53-EV control cells formed the typical neurospheres, silencing TNC in these cells decreased the ability of AGR53 to form these 3D neurosphere structures in stem cell media (Fig. 3a). To confirm the impaired de-differentiation in AGR53-shTNC, we examined the mRNA levels of neural stem cell (NSC)-specific and astrocyte-specific markers by qRT-PCR (Fig. 3b). The results showed reduced levels of NSC markers and higher levels of astrocytes markers in AGR53-shTNC cells compared to the control, suggesting that TNC silencing compromises the ability of the cells to undergo de-differentiation. Tumor cell plasticity is associated with a dynamic cell state and a bidirectional conversion potential between stem and differentiated cell states [30]. Therefore, next we examined the ability of control and 005-shTNC cells to differentiate in response to serum addition in the medium. We found that upon addition of 10% FBS, control 005-EV cells showed elongated processes and expressed more astrocytes and neuron markers (GFAP and Tuj1, respectively) in comparison to the 005-shTNC cells (Fig. 3c, d).

It has been previously shown that tumor derived endothelial cells (TDECs) can originate from glioma stem cells [11, 31]. To further assess if TNC knockdown affects glioma cell plasticity, we tested their capacity to form tumor derived endothelial cells. Since hypoxia is an important factor for TDECs formation [11], we added the iron chelator deferoxamine (DFO) that mimics hypoxia in the culture media. 005 control cells growing in EGM media under hypoxic conditions (either in the presence of DFO or low O_2) significantly changed their morphology to endothelial-like morphology and were able to form tubular structures (Fig. S5a). On the other hand, 005-shTNC growing in the

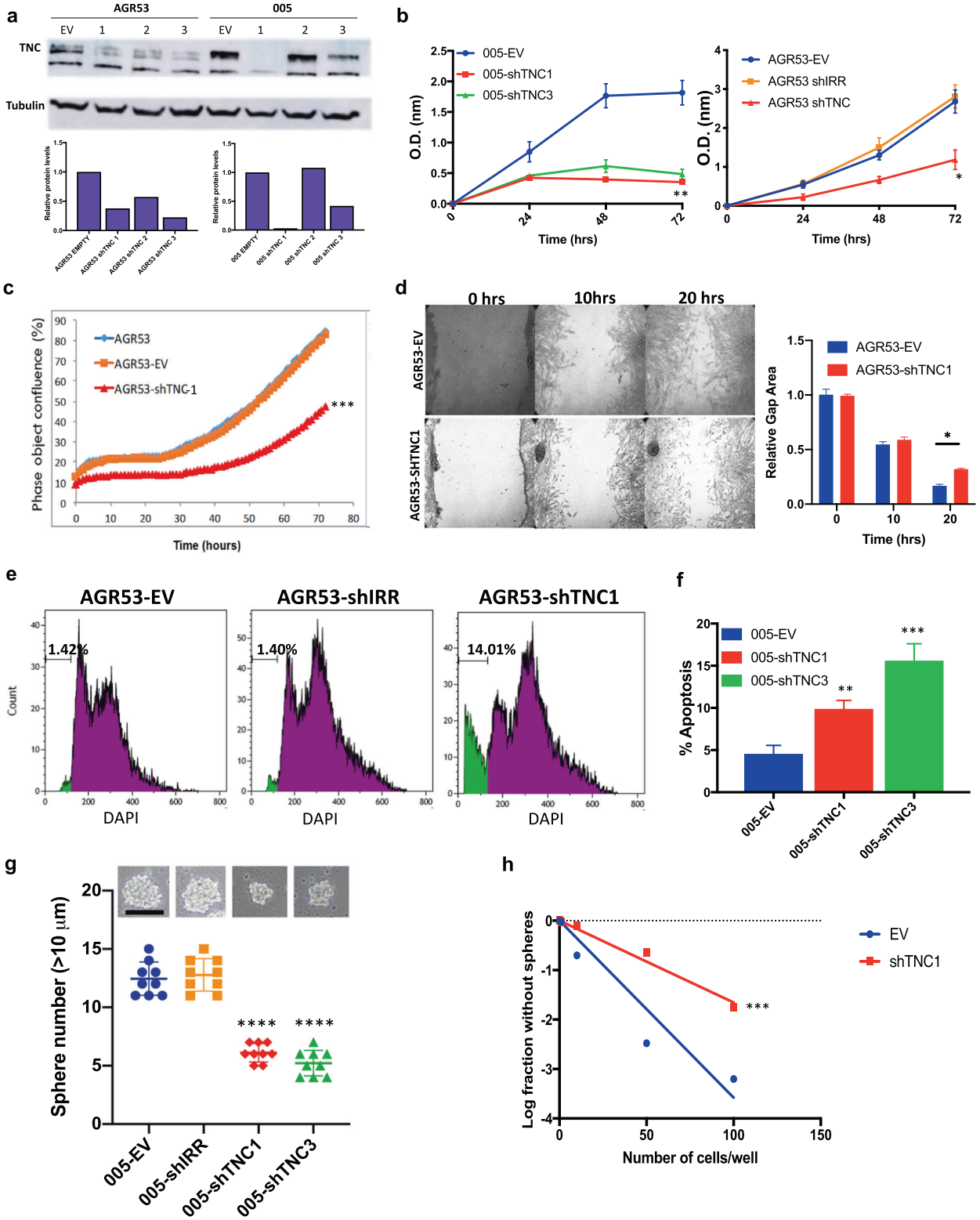

same conditions, although they were able to express markers of endothelial cells (albeit with lower expression and less efficiently; Fig. S5b), were unable to form tube structures when cultured on Matrigel (Fig. 4a).

To gain insights in the mechanism by which TNC supports tumor endothelial differentiation, we examined the literature and came across a previous study that showed high TNC levels in GBM brain tumor initiating cells

◀ **Fig. 2 Silencing TNC reduces glioma cell proliferation and invasion, induces apoptosis and affects stem cell maintenance in vitro.** **a** Western Blot analysis of TNC silencing in AGR53 and 005 glioma cells. Glioma cells were transduced with either an empty vector (EV) or three different shRNAs targeting TNC (shTNC). Tubulin was used as loading control. Graph indicates quantification of western blot analysis. **b** 005 and AGR53 glioma cells were seeded on culture plates ($n = 3$), and WST-1 cell proliferation assay was used to analyze cell proliferation at the indicated time points. 005-EV (005 transduced with empty vector), AGR53 (control), AGR53-shIRR (transduced with control non-targeting shRNA). Error bars represent s.d. of triplicates. Representative of three separate experiments. $^{**}p < 0.01$, $^{*}p < 0.05$. **c** AGR53 (control), AGR53-EV and AGR53-shTNC1 cells were seeded in triplicates and images were taken every hour over a period of 72 h. using the Incucyte system. $^{***}p < 0.001$. **d** Representative images of wound closure of AGR53-EV and AGR53-shTNC1 at the indicated time points. The graph on the right represents the quantification by ImageJ of images taken from three replicates per sample. $^{*}p < 0.05$. Representative of two independent experiments. Assessment of apoptosis by flow cytometry analysis of either AGR53-shTNC1 cell cycle (**e**) or 005-shTNC1 and 3 Annexin V staining (**f**). Error bars represent s.d. $^{**}p < 0.01$, $^{***}p < 0.001$ Representative results of three independent experiments are presented. **g** Effect of shTNC1 and shTNC3 on 005 sphere numbers. A representative image of the tumor spheres for either control or shTNC cells is presented (Top panel), scale bar = 100 µm. The graph quantifies the number of tumor spheres (>10 µm) in EV, shIRR, shTNC1 and shTNC3 infected 005 cells (150 cells per well of a 24-well plate) grown in N2 stem cell media for 5 days. Data are means ± SD (lower panel), $^{****}p < 0.0001$. **h** Effect of shTNC on sphere-forming frequency of 005 glioma stem cells determined by limiting dilution assays. Stem cell frequency was calculated using the extreme limiting dilution analysis (ELDA) software. Data represent means ($n = 12$) $^{***}p < 0.001$. Representative results of two independent experiments.

stimulates NOTCH activity [32]. Going back to our RNA-seq data, we confirmed activation of NOTCH signaling in murine MES GBM (Fig. S6a). NOTCH signaling is a well-conserved pathway which plays a major role in maintenance of the stem cell state in the central nervous system (CNS) [33, 34] and in the regulation of angiogenesis in normal development as well as tumors, including GBM [35–37]. In order to examine the role of NOTCH signaling in TDECs tube formation we repeated the experiment this time in the presence of the γ-secretase inhibitor, DAPT, to block NOTCH signaling (Fig. S6b). As shown in Fig. 4b, inhibition of NOTCH signaling in 005-EV cells decreased tube formation. Finally, TDEC formation is independent of VEGF secretion [11], but other pro-angiogenic factors might be supporting glioma stem cell differentiation to endothelial cells. TNC was shown to induce the secretion of pro-angiogenic factors in GBM cell lines. One of these factors, Ephrin-B2, correlated with TNC expression in GBM, and the inhibition of its receptor (EPHB4) reduced tumor growth and angiogenesis ([20], Fig. S7). 005-shTNC cells expressed reduced levels of *Ephrin-B2* compared to 005-EV control cells, and the incubation of 005 cells with NVP-BHG712, a small tyrosine kinase inhibitor of EPHB4 receptor ([38] and Fig. S8), decreased tube formation (Fig. 4c, d). Altogether, our results suggest a link between TNC expression, Notch activation and Ephrin-B2/EPHB4 interaction and a possible mechanism by which TNC orchestrates tumor derived blood vessel formation.

NF-κB regulates the expression of TNC in GBM

Activation of NF-κB has been involved in multiple aspects of cancer biology, and recent studies showed the link between constitutive activation of NF-κB and MES differentiation in GBM [23, 27]. The transition from proneural to mesenchymal GBM subtype was associated with radioresistant and poor prognosis [27]. As shown in Fig. 1a, b, when we examined the expression of NF-κB target genes, *TNC* was one of the most upregulated genes in our lentiviral-induced MES GBM model. In addition, it has been reported previously that *TNC* promoter has NF-κB binding sites [39]. To further confirm the link between NF-κB activation and TNC expression and functional role, we blocked the NF-κB pathway either using a genetic approach or a small peptide NBD: NEMO (NF-κB essential modifier)–binding domain [40]. We transduced AGR53 cells with a lentiviral vector expressing the IκBαM super repressor and we incubated 005 glioma stem cells with NBDwt peptide, which blocks the interaction of the regulatory protein NEMO with the IKK complex. qRT-PCR analysis confirmed the decreased expression of NF-κB target genes, including *TNC* when using the NBDwt peptide, but not a mutant form of the peptide (NBDmut) that was also used as control (Fig. 5a, b). First, we assessed the ability of the transduced AGR53-IκBαM cells to de-differentiate and form neurosphere-like structures. We observed that while the control AGR53-EV cells form nice neurospheres, the AGR53-IκBαM cells were unable to form these 3-D structures, similar to the results we obtained when TNC was silenced in these cells (Figs. 5c and 3a). The phenotype observed under the microscope was accompanied by the expression of genes mostly associated with an astrocytic signature in the AGR53-IκBαM cells, rather than NSCs specific-genes (Fig. 5d). Next, 005 glioma stem cells were differentiated into endothelial cells, and cultured on Matrigel in the presence of the NBDwt or NBDmut peptide (this short incubation time has no effect on cell viability, see Fig. S9) to evaluate their ability to form endothelial tubes. Similar to 005-shTNC cells, tube formation of 005 cells cultured in the presence of the NBDwt peptide was inhibited compared to the control NBDmut peptide (Fig. 5e). Finally, we were able to reproduce the same results we obtained in a previous study, where orthotopic transplantation of AGR53 expressing the IκBαM super repressor, or mice transplanted with 005 cells and treated with NBDwt peptide, extended mice survival (Fig. S10a, b and [23]). At the end of the 20-day treatment with NBDwt peptide, we

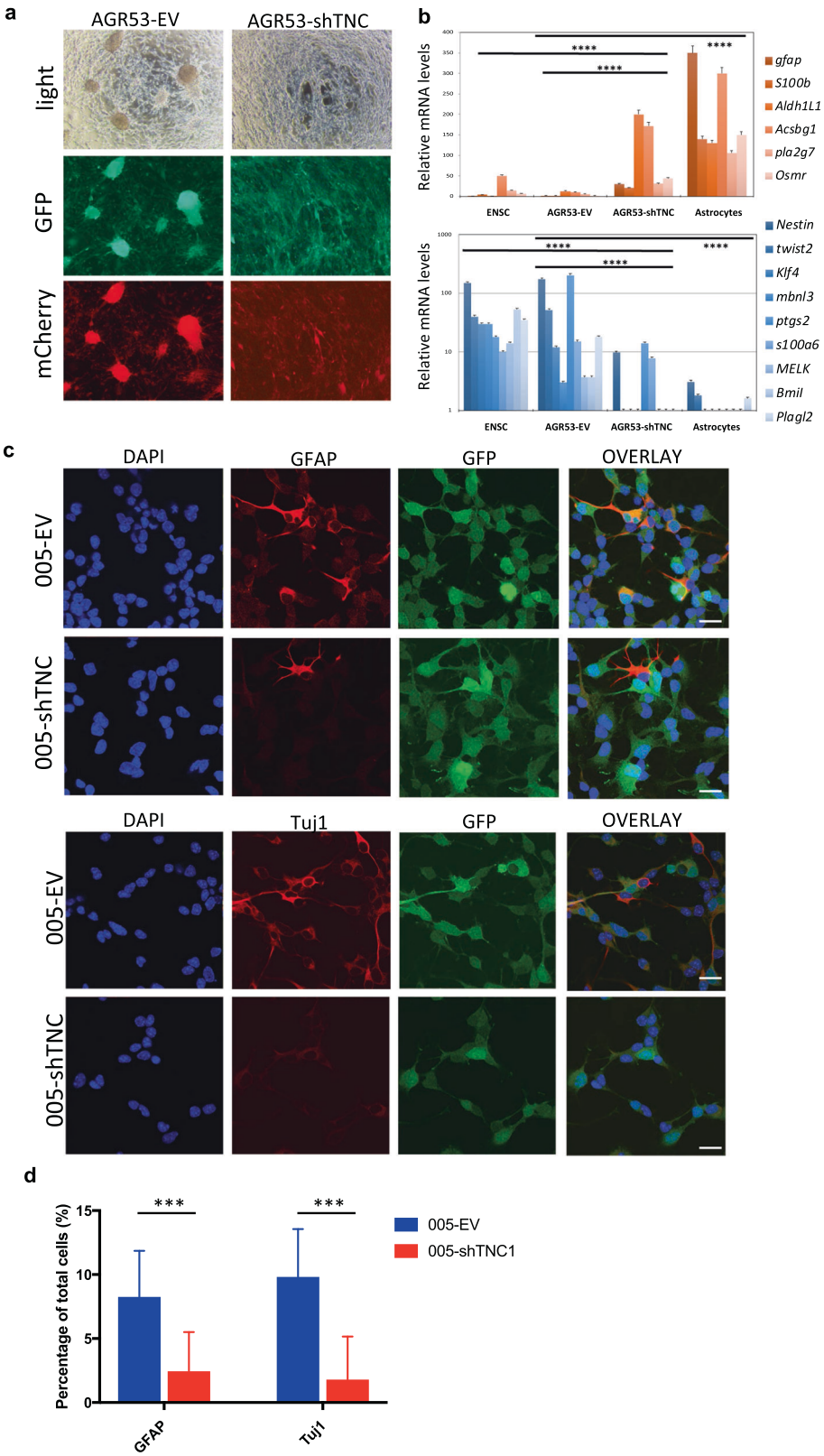

Fig. 3 Depletion of TNC compromises glioma cell plasticity. a Bright field and immunofluorescent images of AGR53-EV and AGR53-shTNC cultured in serum free media supplemented with FGF-2 (N2 stem cell media). GFP = fluorescent reporter of the LV-HRas-shp53 vector; mcherry = reporter of the EV and shTNC vectors. x20 magnification. **b** qRT-PCR analysis of six astrocyte- (top) and nine NSC- (bottom) specific genes in cultured NSC, AGR53-EV and AGR53-shTNC cultured in N2 stem cell media, and primary astrocytes. Gene expression is normalized to the expression of cyclophilin. Error bars represent s.d. ****$p < 0.0001$ Representative of three independent experiments. **c** 005-EV and 005-shTNC cells were cultured in media with the addition of serum (10%) for five days, fixed, stained with GFAP-specific antibody (upper panels) and Tuj-1-specific antibody (lower panels), and observed by confocal microscopy. Magnification x63, Scale bar = 20 µm. The percentage of cells positive for astrocytic or neuronal marker is depicted in **d**. Error bars represent s.d. Five fields analyzed per 3 wells each. ***$p < 0.001$.

sacrificed two mice from the NBDwt treated group and validated by a functional assay (qPCR of NF-κB target genes) that indeed the NBDwt peptide reached the tumors (Fig. S10c). The pleiotropic toxic effect observed with NF-κB inhibitors [23, 41] suggests that downstream targets, such as TNC could serve as possible therapeutic target.

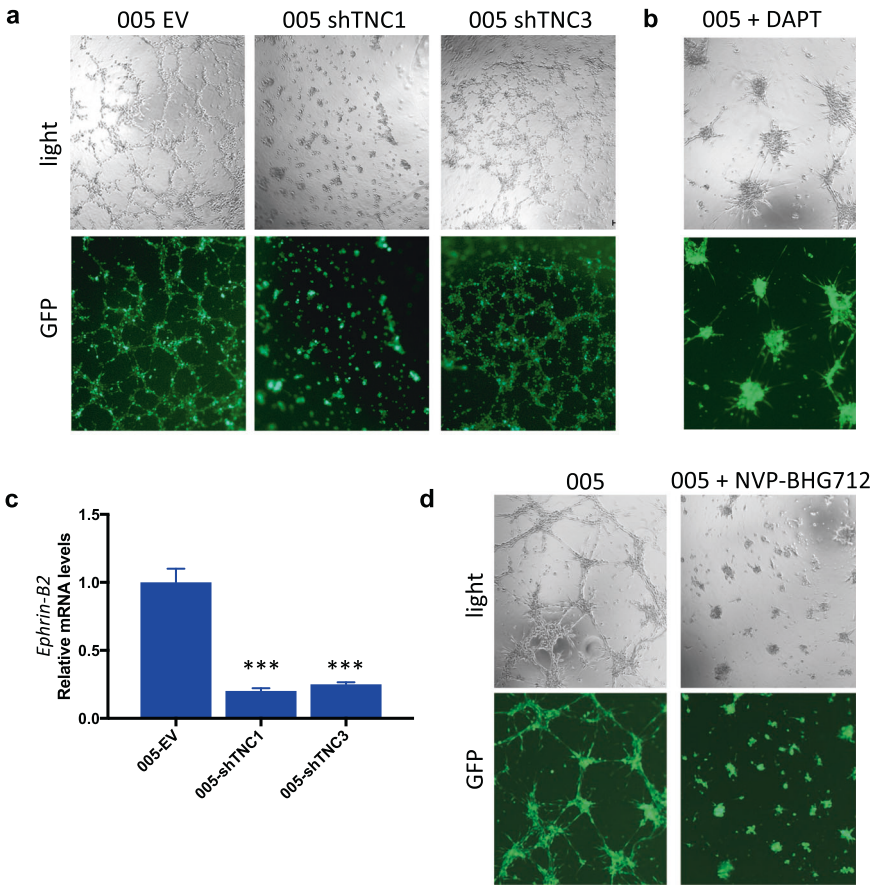

Fig. 4 Silencing TNC impairs endothelial differentiation of glioma stem cells. a, **b** Tube formation assay of 005-EV and 005-shTNC cells cultured in EGM media with DFO and seeded on Matrigel. **b** 005-EV cells were seeded on Matrigel in the absence or presence of the γ-secretase inhibitor DAPT (10 µM). **c** qRT-PCR analysis for Ephrin-B2 expression in 005-EV control and 005-shTNC cells. Gene expression is normalized to the expression of cyclophilin. Error bars represent s.d. ***$p < 0.001$. **d** Tube formation assay of 005 control cells seeded on Matrigel in the absence or presence of EPHB4 inhibitor NVP-BHG712 (500 nM). Representative from two independent experiments.

Disrupting TNC expression in glioma cells inhibits tumor growth

To interrogate the impact of silencing TNC in glioma cells on tumor growth we used intracranial syngeneic mouse models. First, we transplanted AGR53-EV and AGR53-shTNC cells and observed that AGR53-shTNC survived longer than the control group (Fig. S11). Next, control 005-EV glioma stem cells and 005-shTNC were transplanted into syngeneic mouse brains. TNC silencing significantly decreased tumor growth and extended mouse survival (Fig. 6a, b). Interestingly, some of the 005-shTNC transplanted mice never developed tumors. When control 005-EV mice reached end point tumors we sacrificed representative mice from the 005-shTNC group, and analyzed their brains. Confocal microscopy analysis revealed lower expression of Ki67 proliferative marker, suggesting that 005-shTNC tumors proliferate slowly and are probably less invasive and aggressive (Fig. 6c). In addition, qRT-PCR analysis showed that 005-shTNC tumors have decreased expression of MES markers compared to control tumors (Fig. S12). More interestingly, we observed that while 005-EV tumors were highly vascularized, 005-shTNC had much less blood vessels (Fig. 6d). Furthermore, we could not find TDECs in the 005-shTNC tumors, recapitulating the same results we observed in vitro, where silencing TNC compromised the ability of 005 cells to form tube structures (Figs. 6e and 3c). To confirm these results, we also examined dissociated tumors by flow cytometry, and similar to the confocal microscopy observations, the percentage of endothelial cells (CD31+) was higher in control tumors compared to shTNC-tumors, and we could hardly detect TDEC in these tumors (Fig. 6f and Fig. S13).

To further validate the human relevance of our findings, we designed an inducible lentivirus to knockdown TNC (miRTNC) in U87 human GBM (Fig. S14a) [23]. U87 cells transduced with miRTNC were orthotopically injected into the brain of NUDE mice. Ten days after the injection of the cells, one group of mice received doxocyclin (Dox) in their drinking water. The control group continued to drink normal water. As shown in Figs. S14b, c, specific silencing of TNC (miRTNC (+) Dox) significantly decreased tumor growth and prolonged mice survival compared to control miRTNC (-) Dox group. Next, we further validated our results using a patient derived MES glioma stem cell (GBM1005 GSC) and the addition of an mcherry fluorescent reporter to the inducible miRTNC vector (Fig. 7a). In this new version of the vector, transduction of GBM1005 GSC results in concomitant expression of mcherry and knockdown of TNC upon induction with Dox (Fig. S15a, b). GBM1005 GSC

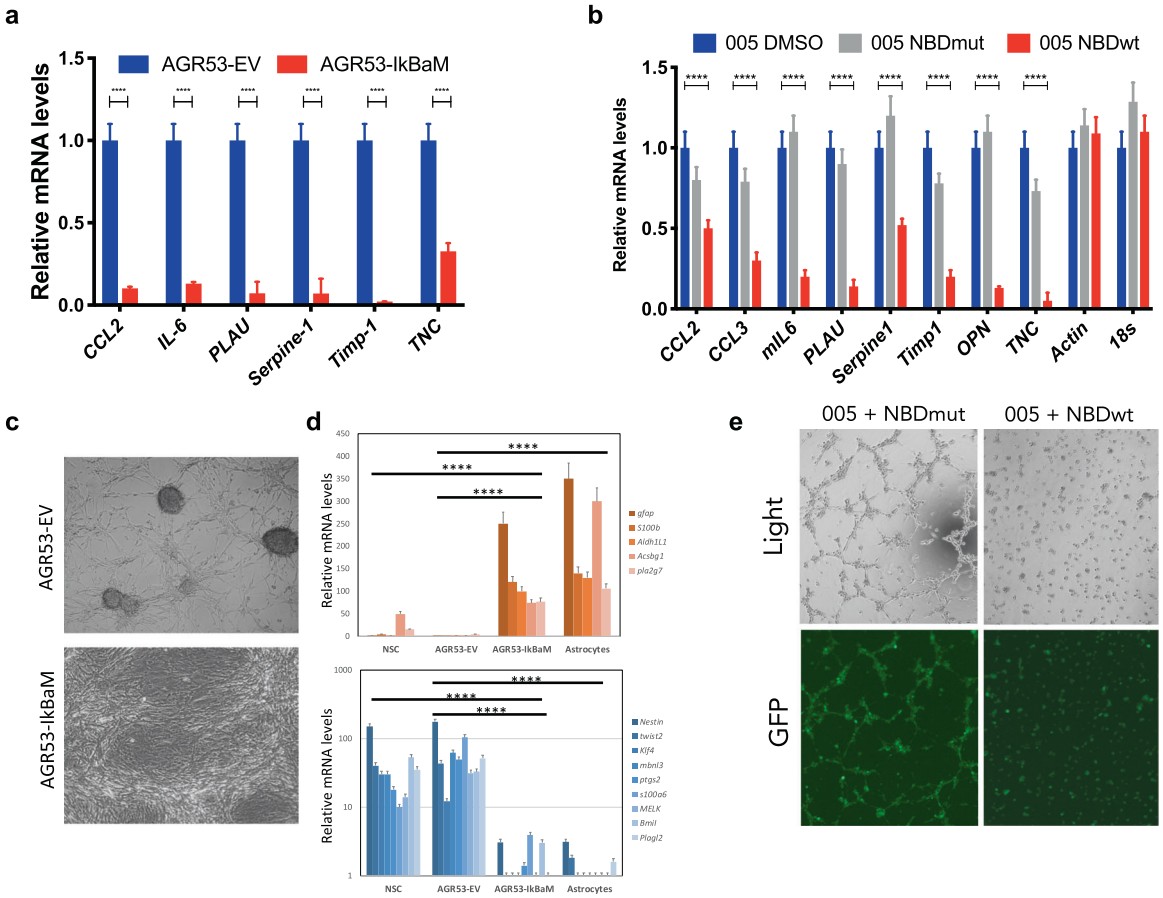

Fig. 5 Blocking NF-κB signaling reduces TNC expression and impairs glioma cell plasticity. a, **b** qRT-PCR analysis of representative NF-κB target genes. **a** AGR53-EV control and AGR53 cells transduced with the IκBαM super repressor (AGR53- IκBαM). **b** 005 cells were incubated with NBDwt (50 μM) or NBDmut (50 μM) peptide for 24 h before qRT-PCR analysis. Gene expression is normalized to the expression of cyclophilin. Data presented as fold change from control. Error bars represent s.d. of technical repeats. $***p < 0.001$, $****p < 0.0001$. **c** Bright field images of AGR53-EV and AGR53-IκBαM cells cultured in serum free media supplemented with FGF-2 (N2 stem cell media). Magnification x20. **d** qRT-PCR analysis of nine NSC- and five astrocyte- specific genes in cultured NSC, AGR53-EV and AGR53- IκBαM cultured in N2 stem cell media, and primary astrocytes. Gene expression is normalized to the expression of cyclophilin. Data presented as fold change from control. Error bars represent s.d. of technical repeats. $****p < 0.0001$. **e** Tube formation assay of 005 cells treated with either NBDmut (50 μM) or NBDwt (50 μM) and subsequently seeded on Matrigel. Representative of three independent experiments.

transduced with either mcherry-miRTNC or mcherry-miRIrr were orthotopically injected in NUDE mice, and in this experiment Dox was given for 15 days by oral gavage. On the last day of the Dox treatment representative mice from each group were sacrificed and knockdown of TNC was confirmed by immunofluorescent staining and confocal microscopy analysis (Fig. 7b). Once more, specific silencing of TNC prolonged mice survival compared to control groups (Fig. 7c). These results are in line with those observed in both glioma patients and GBM patients with IDH1wt status, where down-regulated expression of TNC correlates with better prognosis than patients with up-regulation of TNC (Fig. 7d). Together, our results indicate that silencing TNC conferred prolong survival and further supports the possibility of targeting TNC as a therapeutic approach to glioblastoma treatment.

Discussion

Our study identifies a novel functional role of TNC expressed by the tumor cells and orchestrating glioma cell plasticity. Starting from global analysis of differentially expressed genes in mesenchymal de-differentiated transformed astrocytes and neurons compared to their parental normal cells, we identified *TNC* to be one of the highest expressed genes in the focal adhesion pathway. The focal adhesion pathway caught our attention due to the morphological changes that these cells undergo when they are switched from media that support their differentiated state (flattened shape), to stem cell media that induces the generation of 3D structures known as neurospheres or tumorspheres in cancer [25]. TNC is one of the most abundant components of the extracellular matrix in glioblastoma, and

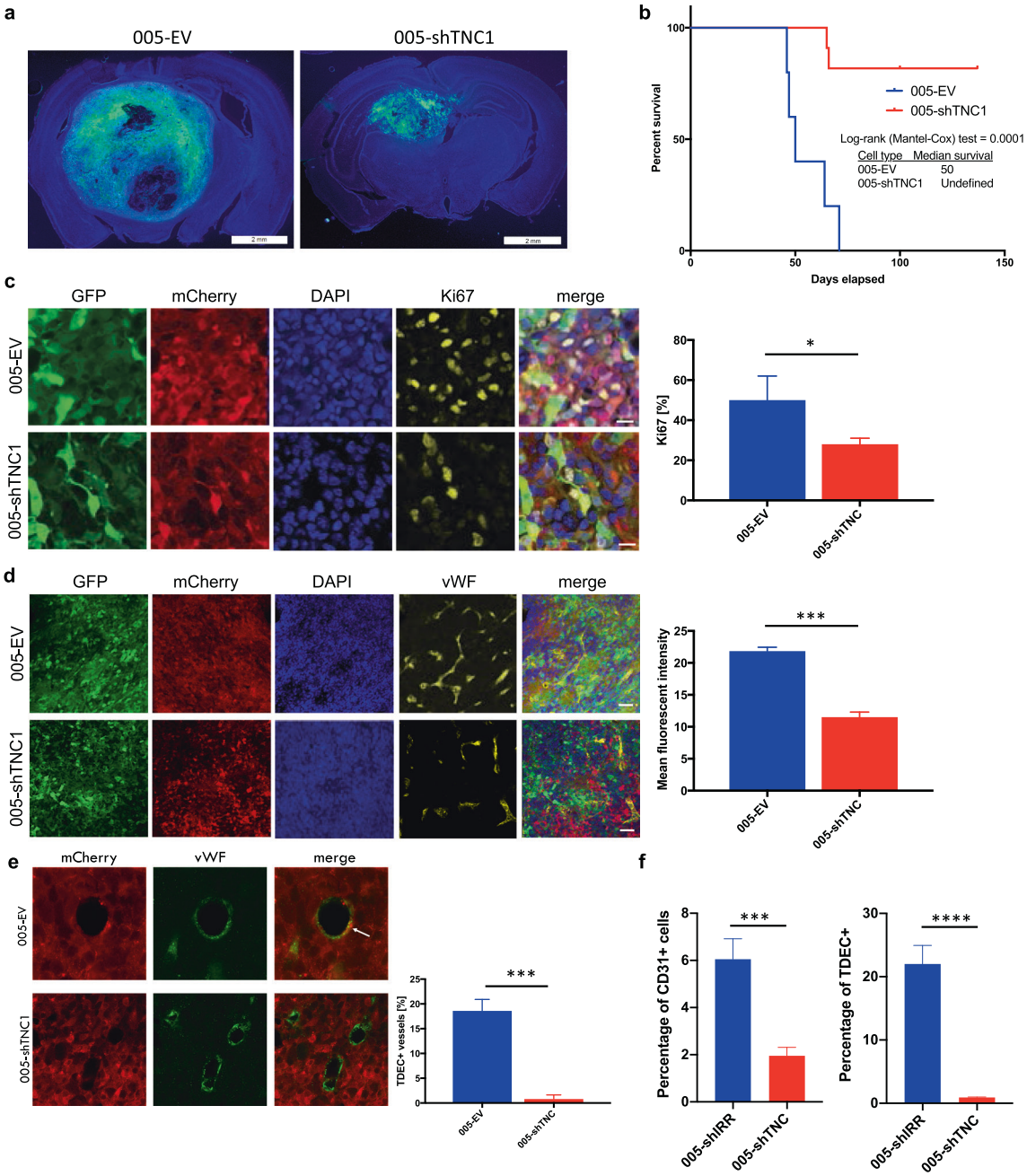

Fig. 6 Silencing TNC suppresses murine 005 tumor growth and reduces blood vessel formation. a Representative fluorescent images of brains collected on day 50 after transplantation of 005-EV or 005-shTNC cells. Scale bars represent 2 mm. **b** Kaplan–Meier survival curves of mice orthotopically transplanted with 005-EV (control) or 005-shTNC cells (3×10^5 cells per mouse; $n = 8$). **c–e** Pictures and quantification of confocal microscopy analysis of tumors collected at the end of the experiment. Brain sections (40 nm) were immunostained with (**c**) Ki67 proliferation marker (Scale bar = 20 µm) and (**d**, **e**) vWF endothelial marker (Scale bar = 50 µm). **e** TDECs (pointed by the arrow) express both mcherry (vector fluorescent reporter in tumor cells) and vWF endothelial marker. $*p < 0.05$, $***p < 0.001$. **f** 005-shIRR (control) and 005-shTNC tumors were dissociated and the CD45-fraction was stained with CD31 antibody and analyzed by flow cytometry. Graphs represent the average of four mice per group ± s.d. The gating strategy is shown in Fig. S13. $***p < 0.001$, $****p < 0.0001$.

indeed its anti-adhesive properties have been previously shown to play a role in GBM neurospheres, facilitating glioma cell migration and invasion [42]. Although TNC is upregulated in malignant gliomas compared to healthy brain tissue, the expression levels are highly associated with the grade of the tumors. High-grade gliomas express higher levels of TNC compared to low and even undetectable levels in low-grade gliomas (LGGs) [43]. Moreover, IDH-1

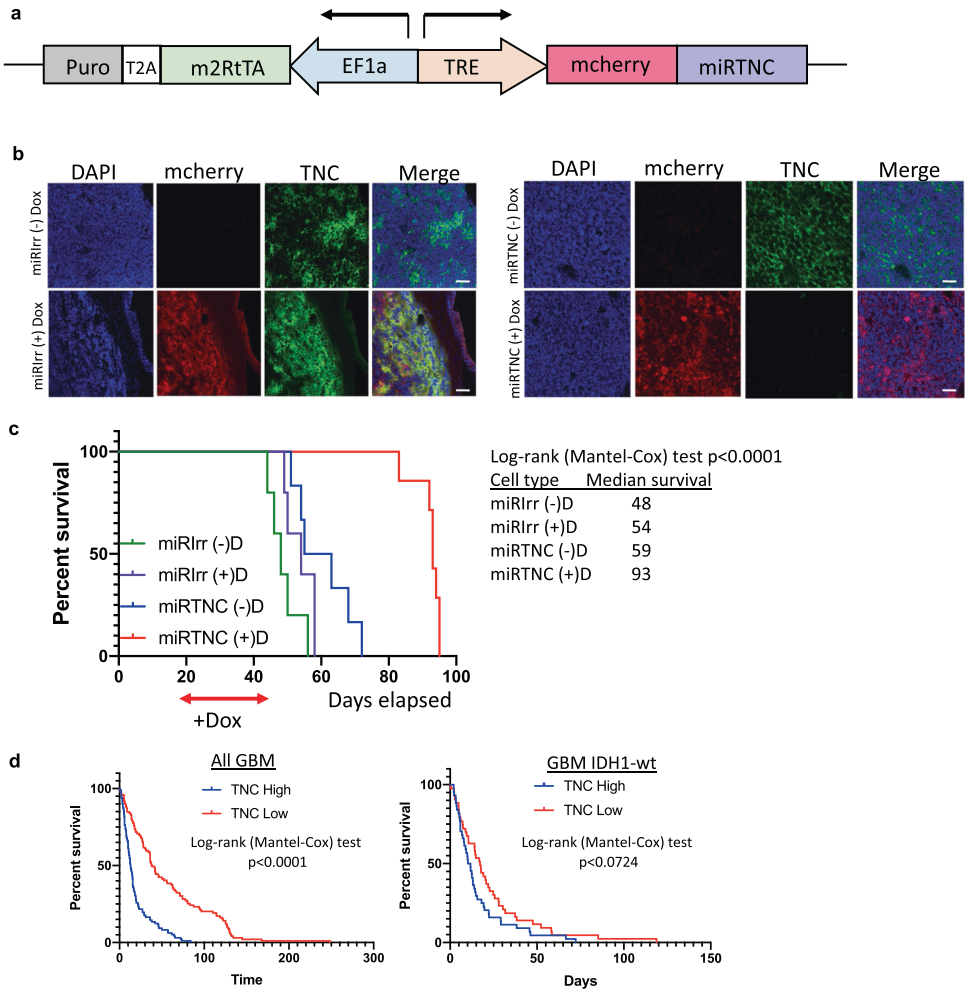

Fig. 7 Specific inhibition of TNC in human GBM-bearing mice improves survival. a Diagram of the inducible shTNC lentiviral vector. The shTNC was cloned following the miR30 backbone under the TRE promoter and preceded by an mcherry fluorescent reporter. The m2rtTA transactivator is expressed from the same vector in the opposite direction under the EF1α promoter and following a T2 A peptide the puromycin gene was placed for selection in vitro. **b** GBM1005 GSC transduced with either miRTNC or miRIrrelevant control (miRIrr) were orthotopically injected (5×10^5/mouse) in NUDE mice ($n = 7$ per group). To induce shTNC or shIrr (and mcherry) expression, mice received Dox (1 mg/ml; 200 µl dose) by oral gavage for 15 days. Representative mice were sacrificed at the last day of Dox administration (or vehicle control) and tumor sections were immunostained with anti-TNC and analyzed by confocal microscope (Scale bar = 50 µm). **c** Kaplan–Meier survival curves of the experiment described in **b**. **d** Kaplan–Meier survival plot for human glioma samples (left graph) and only GBM IDH1wt samples (right graph) with differential *TNC* gene expression (Rembrandt database and GlioVis data tool [51]).

mutant gliomas, which characterize the majority of LGGs and present a better response to radiation therapy and improved prognosis compared to IDH-1 wildtype gliomas, express lower levels of TNC [19]. In this study, we demonstrate that TNC is highly correlated with the most aggressive mesenchymal GBM subtype, both in our murine MES GBM model and human patients (TCGA and Rembrandt databases). Gene expression profiling of bulk GBM and later on single cell analysis, identified different molecular signature subtypes, with PN and MES tumors standing out as being the most consistent subtypes [44]. MES GBM is mostly associated with undifferentiated cells and expression of stem cell markers. Similar to epithelial to mesenchymal transitions (EMT), proneural to mesenchymal transition (PNT) has been found in GBM, even more pronounced in recurrent GBM after conventional chemo and radiotherapy (TCGA data). MES differentiation in GBM is associated with specific gene expression patterns and up-regulation of transcription factors including SNAIL, ZEB1 and TWIST1 [45], as well as STAT3, CEBPB and TAZ [46].

One of the master regulators of MES differentiation is the NF-κB transcription factor. Genetic alterations found in MES tumors, such as loss of NF1 and consequently up-regulation of RAS leads to constitutive activation of NF-κB [47, 48], which in turn regulates transcription factors that promote mesenchymal differentiation [29]. NF-κB activity

has been shown to facilitate the transition of proneural glioma stem cells to MES differentiation [27]. In this study, we show that MES GBM with high NF-κB activity up-regulate the expression of TNC, remodeling and shaping the extracellular matrix (ECM) and hence the microenvironment. Tumor growth and invasion involves remodeling the ECM, and our findings in this study support the idea that tumor cell plasticity also requires these changes. In addition to TNC, we have previously shown that NF-κB regulates the expression of two additional and important components of the ECM, osteopontin (OPN) and Timp1. We showed that OPN is a relevant functional hub in the protein/gene interactome of GBM, and demonstrated that it plays also an important role in de-differentiation of glioma cells [25]. In addition, our search for NF-κB target genes as potential downstream therapeutic targets lead us to Timp1, which we found to be up-regulated in our MES GBM mouse model as well as in human patients. Silencing Timp1 selectively in glioma cells affected their proliferative capacity and prolonged mice survival [23]. Altogether, combining our previous findings and the results from this study, that show decreased levels of TNC when NF-κB signaling is inhibited (Fig. 5a, b), we propose a link between NF-κB activation, expression and secretion of ECM remodeling factors (e.g. OPN, Timp1 and TNC) and glioma cell plasticity. Supporting this notion is the evidence of other important components of the ECM also found to be induced and regulated by NF-κB, such as the proteoglycan, syndecan (SDC1), and enzymes such as the matrix metalloproteases, MMP-2 and MMP-9 [29].

TNC is also a strongly expressed molecule of the AngioMatrix, a signature of angiogenic switch-associated components of the ECM, which correlates with poor prognosis in gliomas and colorectal cancer patients [49]. Indeed, TNC has been shown to play and angio-modulatory role in glioma, by regulating both anti and pro-angiogenic signaling in GBM [20]. In our study, we identified a novel property of TNC, further supporting its role in glioma cell plasticity; the induction of glioma cell differentiation into tumor derived endothelial cells (TDEC). We previously showed that under hypoxic conditions, 005 glioma stem cells could differentiate into TDEC in a VEGF-independent manner [11]. Here we report for the first time, that TNC can induce the expression of EphrinB2, which in turn can bind its receptor, EphB4, and facilitate TDEC formation in an autocrine manner. The paracrine TNC-EphrinB2-EphB4 signaling axis has been previously shown in the context of glioma angiogenesis, which strengthens our current findings [20]. In addition, we believe that the Notch signaling pathway, which is up-regulated in our MES GBM mouse model and patients, is involved in TDEC formation. We showed that the potent γ-secretase inhibitor DAPT compromised the ability of 005 glioma stem cells to generate TDEC and induce tube formation. TNC has been reported to activate Notch signaling and induce tumor angiogenesis [32], but in our study we showed that TNC and Notch signaling contribute to glioma stem cell differentiation into endothelial cells and the formation of tumor derived blood vessels. Finally, our results are in line with previous findings showing that under hypoxic conditions, HIF-1α is induced and it correlates with high levels of TNC. HIF-1α was shown to directly bind to putative hypoxia-response elements in the promoter of TNC [19]. We have shown that 005 glioma stem cells cultured in EGM-2 media + DFO induce the expression of HIF-1α [11], suggesting an important role of HIF-1α in TDEC differentiation and the formation of tubular structures. Here, we add one more important player to the mechanism of TDEC generation, and tumor derived blood vessel formation related to TNC, and suggest EphrinB2 and EphB4 as a potential target axis in GBM anti-angiogenic therapy.

In summary, we suggest that NF-κB activity in MES GBM up-regulates the expression and secretion of TNC, an important component of the glioma ECM. In this study, we propose that TNC can induce glioma cell de-differentiation, support the maintenance and self-renewal of glioma stem cells, and facilitate their differentiation, under hypoxic conditions, to tumor derived endothelial cells. The extracellular matrix, and TNC as one of its components, has been shown to be involved in mediating stem cell fate [50]. Here, we support the old and established notion that cancer cells "hijack" normal programs, and show that by remodeling the ECM and up-regulating the expression of TNC, gliomas facilitate tumor cell plasticity and hence tumor growth, aggressiveness, and invasion. Our findings suggest that TNC, an abundant ECM component in GBM, provides a promising target for therapeutic intervention aimed at disabling glioma cell plasticity and improve the prognosis of glioma patients.

Acknowledgements We thank Yifeng Xia and Eugene Ke for assistance in bioinformatic analysis, and Prof. Michal Baniyash for critically reading the manuscript. This research was supported by grants to DF-M from the Israel Science Foundation (Grant no. 1310/15), the Israel Cancer Research Fund (Research Career Development Award), and the EU-FP7 Marie Curie Actions (Career Integration Grant).

Author contributions DF-M designed the research, IA, OPK, LRN and DFM performed the experiments, IA and DFM analyzed the results, IA and DFM wrote the manuscript

Compliance with ethical standards

Conflict of interest The authors declare that they have no conflict of interest.

Publisher's note Springer Nature remains neutral with regard to jurisdictional claims in published maps and institutional affiliations.

References

1. Furnari FB, Fenton T, Bachoo RM, Mukasa A, Stommel JM, Stegh A, et al. Malignant astrocytic glioma: genetics, biology, and paths to treatment. Genes Dev. 2007;21:2683–710.
2. Friedmann-Morvinski D. Glioblastoma heterogeneity and cancer cell plasticity. Crit Rev Oncog. 2014;19:327–36.
3. Phillips HS, Kharbanda S, Chen R, Forrest WF, Soriano RH, Wu TD, et al. Molecular subclasses of high-grade glioma predict prognosis, delineate a pattern of disease progression, and resemble stages in neurogenesis. Cancer Cell. 2006;9:157–73.
4. Verhaak RG, Hoadley KA, Purdom E, Wang V, Qi Y, Wilkerson MD, et al. Integrated genomic analysis identifies clinically relevant subtypes of glioblastoma characterized by abnormalities in PDGFRA, IDH1, EGFR, and NF1. Cancer Cell. 2010;17:98–110.
5. Friedmann-Morvinski D, Verma IM. Dedifferentiation and reprogramming: origins of cancer stem cells. EMBO Rep. 2014;15:244–53.
6. Chaffer CL, Marjanovic ND, Lee T, Bell G, Kleer CG, Reinhardt F, et al. Poised chromatin at the ZEB1 promoter enables breast cancer cell plasticity and enhances tumorigenicity. Cell. 2013;154:61–74.
7. Ischenko I, Zhi J, Moll UM, Nemajerova A, Petrenko O. Direct reprogramming by oncogenic Ras and Myc. Proc Natl Acad Sci USA. 2013;110:3937–42.
8. Mani SA, Guo W, Liao MJ, Eaton EN, Ayyanan A, Zhou AY, et al. The epithelial-mesenchymal transition generates cells with properties of stem cells. Cell. 2008;133:704–15.
9. Schwitalla S, Fingerle AA, Cammareri P, Nebelsiek T, Goktuna SI, Ziegler PK, et al. Intestinal tumorigenesis initiated by dedifferentiation and acquisition of stem-cell-like properties. Cell. 2013;152:25–38.
10. Friedmann-Morvinski D, Bushong EA, Ke E, Soda Y, Marumoto T, Singer O, et al. Dedifferentiation of neurons and astrocytes by oncogenes can induce gliomas in mice. Science. 2012;338:1080–4.
11. Soda Y, Marumoto T, Friedmann-Morvinski D, Soda M, Liu F, Michiue H, et al. Transdifferentiation of glioblastoma cells into vascular endothelial cells. Proc Natl Acad Sci USA. 2011;108:4274–80.
12. Poltavets V, Kochetkova M, Pitson SM, Samuel MS. The role of the extracellular matrix and its molecular and cellular regulators in cancer cell plasticity. Front Oncol. 2018;8:431.
13. Midwood KS, Chiquet M, Tucker RP, Orend G. Tenascin-C at a glance. J Cell Sci. 2016;129:4321–7.
14. Chiquet-Ehrismann R, Orend G, Chiquet M, Tucker RP, Midwood KS. Tenascins in stem cell niches. Matrix Biol. 2014;37:112–23.
15. Brosicke N, Faissner A. Role of tenascins in the ECM of gliomas. Cell Adh Migr. 2015;9:131–40.
16. Lowy CM, Oskarsson T. Tenascin C in metastasis: a view from the invasive front. Cell Adh Migr. 2015;9:112–24.
17. Midwood KS, Hussenet T, Langlois B, Orend G. Advances in tenascin-C biology. Cell Mol Life Sci. 2011;68:3175–99.
18. Yoshida T, Akatsuka T, Imanaka-Yoshida K. Tenascin-C and integrins in cancer. Cell Adh Migr. 2015;9:96–104.
19. Miroshnikova YA, Mouw JK, Barnes JM, Pickup MW, Lakins JN, Kim Y, et al. Tissue mechanics promote IDH1-dependent HIF1alpha-tenascin C feedback to regulate glioblastoma aggression. Nat Cell Biol. 2016;18:1336–45.
20. Rupp T, Langlois B, Koczorowska MM, Radwanska A, Sun Z, Hussenet T, et al. Tenascin-C orchestrates glioblastoma angiogenesis by modulation of pro- and anti-angiogenic signaling. Cell Rep. 2016;17:2607–19.
21. Marumoto T, Tashiro A, Friedmann-Morvinski D, Scadeng M, Soda Y, Gage FH, et al. Development of a novel mouse glioma model using lentiviral vectors. Nat Med. 2009;15:110–6.
22. Dull T, Zufferey R, Kelly M, Mandel RJ, Nguyen M, Trono D, et al. A third-generation lentivirus vector with a conditional packaging system. J Virol. 1998;72:8463–71.
23. Friedmann-Morvinski D, Narasimamurthy R, Xia Y, Myskiw C, Soda Y, Verma IM. Targeting NF-kappaB in glioblastoma: a therapeutic approach. Sci Adv. 2016;2:e1501292.
24. Zuber J, McJunkin K, Fellmann C, Dow LE, Taylor MJ, Hannon GJ, et al. Toolkit for evaluating genes required for proliferation and survival using tetracycline-regulated RNAi. Nat Biotechnol. 2011;29:79–83.
25. Friedmann-Morvinski D, Bhargava V, Gupta S, Verma IM, Subramaniam S. Identification of therapeutic targets for glioblastoma by network analysis. Oncogene. 2015;35:608–20.
26. Saito N, Fu J, Zheng S, Yao J, Wang S, Liu DD, et al. A high Notch pathway activation predicts response to gamma secretase inhibitors in proneural subtype of glioma tumor-initiating cells. Stem Cells. 2014;32:301–12.
27. Bhat KP, Balasubramaniyan V, Vaillant B, Ezhilarasan R, Hummelink K, Hollingsworth F, et al. Mesenchymal differentiation mediated by NF-kappaB promotes radiation resistance in glioblastoma. Cancer Cell. 2013;24:331–46.
28. Thiery JP. Epithelial-mesenchymal transitions in tumour progression. Nat Rev Cancer. 2002;2:442–54.
29. Yamini B. NF-kappaB, mesenchymal differentiation and glioblastoma. Cells. 2018;7:125–43.
30. Cabrera MC, Hollingsworth RE, Hurt EM. Cancer stem cell plasticity and tumor hierarchy. World J Stem Cells. 2015;7:27–36.
31. Ricci-Vitiani L, Pallini R, Biffoni M, Todaro M, Invernici G, Cenci T, et al. Tumour vascularization via endothelial differentiation of glioblastoma stem-like cells. Nature. 2010;468:824–8.
32. Sarkar S, Mirzaei R, Zemp FJ, Wei W, Senger DL, Robbins SM, et al. Activation of NOTCH signaling by tenascin-C promotes growth of human brain tumor-initiating cells. Cancer Res. 2017;77:3231–43.
33. Androutsellis-Theotokis A, Leker RR, Soldner F, Hoeppner DJ, Ravin R, Poser SW, et al. Notch signalling regulates stem cell numbers in vitro and in vivo. Nature. 2006;442:823–6.
34. Shen Q, Goderie SK, Jin L, Karanth N, Sun Y, Abramova N, et al. Endothelial cells stimulate self-renewal and expand neurogenesis of neural stem cells. Science. 2004;304:1338–40.
35. Dufraine J, Funahashi Y, Kitajewski J. Notch signaling regulates tumor angiogenesis by diverse mechanisms. Oncogene. 2008;27:5132–7.
36. Gridley T. Notch signaling in vascular development and physiology. Development. 2007;134:2709–18.
37. Hovinga KE, Shimizu F, Wang R, Panagiotakos G, Van Der Heijden M, Moayedpardazi H, et al. Inhibition of notch signaling in glioblastoma targets cancer stem cells via an endothelial cell intermediate. Stem Cells. 2010;28:1019–29.
38. Martiny-Baron G, Holzer P, Billy E, Schnell C, Brueggen J, Ferretti M, et al. The small molecule specific EphB4 kinase inhibitor NVP-BHG712 inhibits VEGF driven angiogenesis. Angiogenesis. 2010;13:259–67.
39. Mettouchi A, Cabon F, Montreau N, Dejong V, Vernier P, Gherzi R, et al. The c-Jun-induced transformation process involves complex regulation of tenascin-C expression. Mol Cell Biol. 1997;17:3202–9.
40. May MJ, D'Acquisto F, Madge LA, Glockner J, Pober JS, Ghosh S. Selective inhibition of NF-kappaB activation by a peptide that blocks the interaction of NEMO with the IkappaB kinase complex. Science. 2000;289:1550–4.
41. Bottero V, Withoff S, Verma IM. NF-kappaB and the regulation of hematopoiesis. Cell Death Differ. 2006;13:785–97.
42. Xia S, Lal B, Tung B, Wang S, Goodwin CR, Laterra J. Tumor microenvironment tenascin-C promotes glioblastoma invasion and negatively regulates tumor proliferation. Neuro Oncol. 2016;18:507–17.
43. Nie S, Gurrea M, Zhu J, Thakolwiboon S, Heth JA, Muraszko KM, et al. Tenascin-C: a novel candidate marker for cancer stem cells in glioblastoma identified by tissue microarrays. J Proteome Res. 2015;14:814–22.

44. Huse JT, Phillips HS, Brennan CW. Molecular subclassification of diffuse gliomas: seeing order in the chaos. Glia. 2011;59:1190–9.
45. Nieto MA, Huang RY, Jackson RA, Thiery JP. Emt: 2016. Cell. 2016;166:21–45.
46. Carro MS, Lim WK, Alvarez MJ, Bollo RJ, Zhao X, Snyder EY, et al. The transcriptional network for mesenchymal transformation of brain tumours. Nature. 2010;463:318–25.
47. Finco TS, Westwick JK, Norris JL, Beg AA, Der CJ, Baldwin AS Jr. Oncogenic Ha-Ras-induced signaling activates NF-kappaB transcriptional activity, which is required for cellular transformation. J Biol Chem. 1997;272:24113–6.
48. Mayo MW, Wang CY, Cogswell PC, Rogers-Graham KS, Lowe SW, Der CJ, et al. Requirement of NF-kappaB activation to suppress p53-independent apoptosis induced by oncogenic Ras. Science. 1997;278:1812–5.
49. Langlois B, Saupe F, Rupp T, Arnold C, van der Heyden M, Orend G, et al. AngioMatrix, a signature of the tumor angiogenic switch-specific matrisome, correlates with poor prognosis for glioma and colorectal cancer patients. Oncotarget. 2014;5:10529–45.
50. Garcion E, Halilagic A, Faissner A, ffrench-Constant C. Generation of an environmental niche for neural stem cell development by the extracellular matrix molecule tenascin C. Development. 2004;131:3423–32.
51. Bowman RL, Wang Q, Carro A, Verhaak RG, Squatrito M. GlioVis data portal for visualization and analysis of brain tumor expression datasets. Neuro Oncol. 2017;19:139–41.